

## Critical Shape and Size for Dislocation Nucleation in $\text{Si}_{1-x}\text{Ge}_x$ Islands on Si(001)

A. Marzegalli,<sup>1</sup> V. A. Zinovyev,<sup>1,†</sup> F. Montalenti,<sup>1</sup> A. Rastelli,<sup>2,3</sup> M. Stoffel,<sup>2</sup> T. Merdzhanova,<sup>2</sup>  
O. G. Schmidt,<sup>2,3</sup> and Leo Miglio<sup>1,\*</sup>

<sup>1</sup>*L-NESS and Dipartimento di Scienza dei Materiali, Università degli Studi di Milano-Bicocca, via Cozzi 53, I-20125 Milano, Italy*

<sup>2</sup>*Max-Planck-Institut für Festkörperforschung, Heisenbergstraße 1, 70569 Stuttgart, Germany*

<sup>3</sup>*Institute for Integrative Nanosciences, IFW Dresden, Helmholtzstrasse 20, 01069 Dresden, Germany*

(Received 7 May 2007; published 7 December 2007)

The critical volume for the onset of plastic strain relaxation in SiGe islands on Si(001) is computed for different Ge contents and realistic shapes by using a three-dimensional model, with position-dependent dislocation energy. It turns out that the critical bases for dome- and barnlike islands are different for any composition. By comparison to extensive atomic force microscopy measurements of the footprints left on the Si substrates by islands grown at different temperatures (and compositions), we conclude that, in contrast with planar films, dislocation nucleation in 3D islands is fully thermodynamic.

DOI: [10.1103/PhysRevLett.99.235505](https://doi.org/10.1103/PhysRevLett.99.235505)

PACS numbers: 61.72.Bb, 68.37.Ps, 81.07.-b, 81.15.Hi

Molecular beam epitaxy (MBE) of Ge on Si(001) at common (500–800 °C) temperatures proceeds in a Stranski-Krastanow fashion [1]: after the formation of a thin pseudomorphic wetting layer (WL), coherent three-dimensional islands appear on the substrate. As the Ge deposition increases, islands change from shallow (prepyramids and pyramids) to steeper (domes and barns) morphologies [2–4], according to a larger strain relaxation and to a reduction in surface to volume ratio. By plotting the aspect ratio  $r$  (i.e., the height to base ratio) with the volume of the islands grown at 700 °C [5] a rapid increase occurs, particularly for domes and barns, the former being characterized by  $0.18 \leq r \leq 0.23$ , the latter at  $0.23 \leq r \leq 0.35$ . At the same time, the deposited Ge partially mixes with Si from the substrate, mainly via surface diffusion, leading to islands having a Ge fraction decreasing with increasing growth temperatures, both in chemical vapor deposition [6] and MBE growth [5,7]. Such an alloying is driven by the entropy of mixing [8] and by the elastic strain reduction, also competing with the plastic strain relaxation by dislocations, which is the common mechanism in continuous and Ge-diluted films [9]. Actually, for large Ge coverages, the islands reach some critical volume, and plastic relaxation occurs in any case. Then, the island growth proceeds in a discontinuous and cyclic way, periodically lowering  $r$  each time a new dislocation is introduced. This phenomenon was observed by real time transmission electron microscopy (TEM) *in situ* [10,11] and deduced from the atomic force microscopy (AFM) analysis of the “footprints” left by dislocated islands on the Si substrate [12,13] after selective wet chemical etching of the SiGe epilayer. The latter approach allows us to determine accurately the critical base size for the introduction of the first dislocation, but does not tell which was the actual shape (dome or barn) at the very critical volume. Such an information cannot be easily extracted from AFM images before etching, since the nucleation of the first dislocation is readily followed by a change in shape to dislocated domes

(superdomes), with a lowering of the aspect ratio [10]. Therefore, it is important to have a quantitative model relating the base size of a critical island to its shape and to its average composition.

Because of the linear superposition of the elastic field of the dislocation to the inhomogeneous strain distribution in the coherent island, the critical volume is determined by equating the energy cost for introducing one dislocation  $E_{\text{cost}}$  (i.e., the distortion energy produced by the dislocation itself in a fully relaxed island) to the energy gain produced by the dislocation in a strained island  $E_{\text{gain}}$  (i.e., the interaction energy between the inhomogeneous misfit stress in the island and the strain field of the dislocation itself). In the last ten years, only a few authors attempted the prediction of the critical size for heteroepitaxial islands, with different approximations to the scheme above, unfortunately in two dimensions [14] or simplified island shape [15].

In this Letter we propose a three-dimensional model that fully takes into account both the position-dependent  $E_{\text{gain}}$  via a finite element method (FEM) calculation and analytic  $E_{\text{cost}}$  at that precise location, for realistic dome and barn shapes, at any size and composition.

Figure 1(a) shows the actual dome geometry used in our FEM calculation, with typical  $\{15\ 3\ 23\}$ ,  $\{113\}$ ,  $\{105\}$ , and  $\{001\}$  facets [2]. In Fig. 2(a) we display the barn geometry that we have considered. It is constructed following the experimentally observed shape [4]: the facets are  $\{111\}$ ,  $\{20\ 4\ 23\}$ ,  $\{113\}$ ,  $\{15\ 3\ 23\}$ ,  $\{105\}$ , and  $\{001\}$ . In the figure, the  $x$  and  $y$  axes are oriented in the  $[-110]$ ,  $[110]$  crystallographic directions, respectively, and the origin of the coordinates is placed at the base center. In Figs. 1(b) and 2(b) we report the FEM predictions of the stress component  $\sigma_{xx}$  for pure-Ge domes and barns, respectively, as calculated at the cross section located at  $y = 0$ . We see that the higher aspect ratio of the latter accounts for a larger stress release.

According to Ref. [16],  $E_{\text{gain}}$  can be obtained using the Peach-Koeler force [17] describing the interaction between

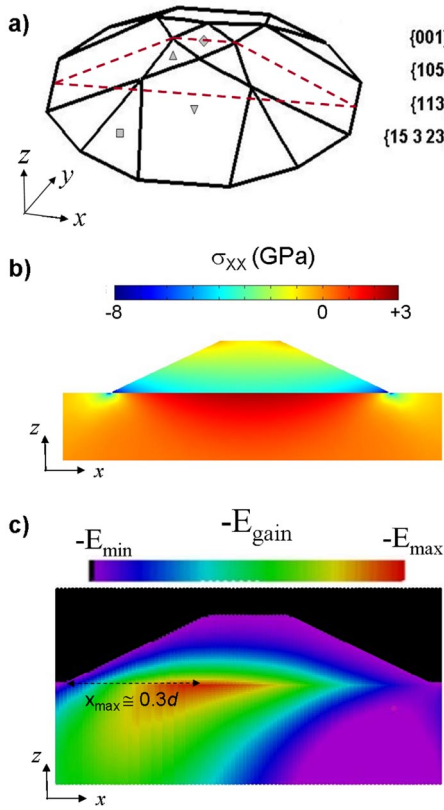


FIG. 1 (color online). (a) 3D view of the dome-shaped island used for the FEM calculations. (b) Cross section of the  $\sigma_{xx}$  3D map taken perpendicular to the [110] direction in the case of a Ge-pure dome. (c) Color map of the relative energy gain, so that the map is self-similar with volume and composition.

a dislocation of Burgers vector  $\vec{b}$  ( $b = 0.38$  nm for Si and  $0.39$  nm for Ge) and dislocation line  $\vec{l}$  with the existing elastic stress tensor  $\hat{\sigma}$ :  $\vec{F} = \vec{b} \cdot \hat{\sigma} \times \vec{l}$ .

Typical dislocations in zinc blende structures (60 degrees in type [17]) run along the  $\{110\}$  directions with  $\vec{b} = \frac{a}{2} \times \langle 011 \rangle$ . Therefore, we place the dislocation line  $\vec{l}$  parallel to the  $y$  axis. Consequently, the work performed to place a misfit dislocation line in any position  $(x_0, z_0)$  of the island is

$$E_{\text{gain}}(x_0, z_0) = \left[ b_x \int_{z_0}^{h(x_0, z_0)} \left( \int_{l(x_0, z)} \sigma_{xx} dy \right) dz + b_z \int_{z_0}^{h(x_0, z_0)} \left( \int_{l(x_0, z)} \sigma_{xz} dy \right) dz \right], \quad (1)$$

where  $h(x_0, z_0)$  is the distance of the  $(x_0, z_0)$  position from the free surface along  $z$ ,  $l(x_0, z)$  is the dislocation line length along  $y$ , which depends on  $z$  in a different way for domes and barns. As usual,  $b_x$ ,  $b_z$  are the components of the Burgers vector in the  $[-110]$  and in the  $[001]$  directions, respectively. The integral of the Peach-Koeler force is path independent, if the stress field is calculated at the equilibrium, so that it is possible to calculate it along a

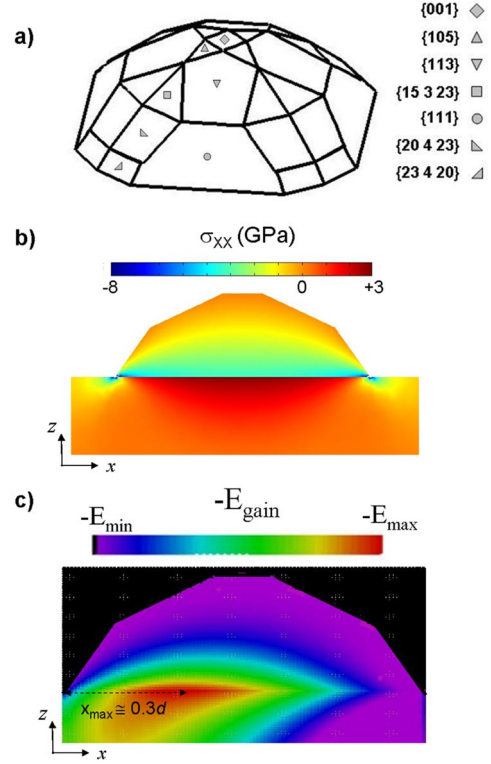


FIG. 2 (color online). The same as Fig. 2 for the barn shape.

straight vertical path, from the surface to each location in the system.

In Figs. 1(c) and 2(c) we report a color-scale mapping of the relative  $E_{\text{gain}}(x, z)$  for domes and barns, which is valid for any size and average composition. For both shapes the largest energy gain (about  $14$  eV/nm for a Ge-pure dome) is obtained at  $(x_0, 0)$ , i.e., at a distance from the island edge of  $0.3d$  ( $d$  is the width of the island base). The left side of the islands in Figs. 1 and 2 is the preferential site for Burgers vector along  $[011]$ , whereas it is symmetrically placed on the right side for the Burgers vector oriented along  $[0\bar{1}1]$ . Our prediction agrees with the one of Spencer and Tersoff [16] for the case of an infinitely elongated island along  $y$ , and does not change significantly if  $E_{\text{cost}}$  is added to  $E_{\text{gain}}$ .

The classical elasticity theory for continuous flat films provides an analytical expression for the energy cost as the one stored in a cylinder around a dislocation line of length  $l$  and radius  $R$  as large as the film thickness or half the distance between two parallel dislocations [9]. By disregarding the contributions arising from the terminations of the dislocation line at the island base perimeter, we just remain with the problem of estimating the atomistic contribution of the dislocation core (bond-breaking originated) and the one of selecting an effective  $\bar{R}$ , suitable for the island geometry.

According to Refs. [15,17] and to a very recent calculation for SiGe alloys [18], we include the former in the analytical expression for the elastic energy, which gives

$$E_{\text{cost}}(x_0, z_0) = l(x_0, z_0) \frac{1}{2\pi} \frac{\mu_{\text{Si}} \mu_{\text{SiGe}}}{\mu_{\text{Si}} + \mu_{\text{SiGe}}} \times b^2 \left[ \cos^2 \beta + \frac{\sin^2 \beta}{1 - \nu_{\text{SiGe}}} \right] \left( \ln \frac{\bar{R}}{b} + 1 \right), \quad (2)$$

where  $\mu$  is the shear modulus and  $\nu$  is the Poisson ratio.  $\bar{R}$  is taken, as successfully proposed in [15], to be the geometric average of the distances of the dislocation line from the base edge and the free surface above, as calculated in the middle cross section of the island, where they take the maximum value for any  $y$ . Such apparently rough approximation does not affect critically the estimation of  $E_{\text{cost}}$ , since for island base sizes of our interest, i.e., 50–150 nm,  $\bar{R}/b$  in the optimised position for  $E_{\text{gain}}$  varies between 40 and 100, respectively. Therefore, even increasing  $\bar{R}$  by 50% in Eq. (2), gives rise to a variation in  $E_{\text{cost}}$  between 9% and 7%, corresponding to a modification in the critical base by 14% at maximum. We obtain the critical island size at fixed average composition (i.e., average misfit in the FEM approach) by numerically computing the energy gain and analytically estimating the energy cost for different island dimensions and dislocation positions along the island base, and determining the volume at which they are equal. This procedure is iterated for any homogeneous distribution of the Ge content for domes and barns, from 20% up to 70%, every 10%. Realistic inhomogeneous Ge distributions have been also checked to provide variations in the critical base size of less than 3% for 70% Ge average composition, in the case of two dimensional ridges with a dome cross section, investigated by a full FEM calculation including the dislocation field (still in progress, see [19]).

In order to experimentally estimate the critical size for the first dislocation nucleation as a function of island composition we deposit 15 monolayers of Ge on Si(001), at temperatures between 620 and 800 °C using solid source MBE. Coherent islands with barn shape and large dislocated islands are observed in the whole temperature range. The SiGe material is then removed by selective wet chemical etching following the procedure described in Ref. [13]. This enables us to study by AFM the tree-ring structure left by islands on the Si substrate during the cyclic growth (insets in Fig. 3). The central Si plateau can be interpreted as the original island base prior to introduction of the first dislocation. Its size can thus be taken as a measure of the critical diameter  $d$  for dislocation introduction, at a given temperature [inset of Fig. 3(c)]. The statistical analysis of the critical plateau size  $d$  obtained from extensive measurements on samples grown at four different temperatures is shown in Fig. 3 along with representative AFM images. The average Ge content of islands grown at different temperatures is determined by measuring the total volume of material per unit area from the AFM images and comparing it with the nominally deposited Ge amount [13].

In Fig. 4 we report  $d$  averaged over more than hundred islands (full circles) as a function of the average Ge content

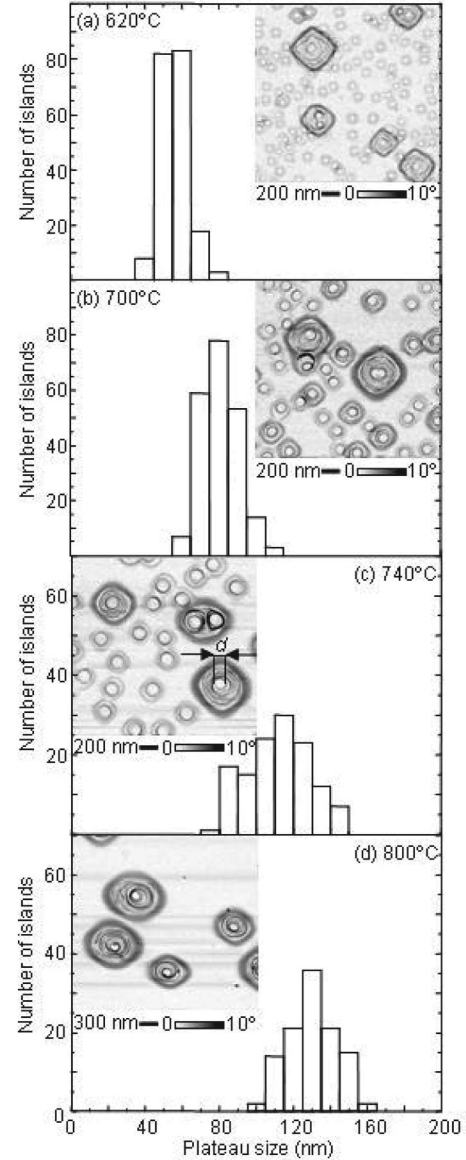


FIG. 3. Statistical analysis of the critical size for islands obtained by depositing 15 ML Ge on Si(001) substrates at 620 (a), 700 (b), 740 (c), and 800 °C (d). The critical size  $d$  is assumed to be equal to the width of the central plateau of the tree-ring structure buried below SiGe superdomes and revealed by selective removal of the SiGe epilayer (see AFM insets). AFM images taken prior to selective etching show that coherent islands have the shape of barns for all the employed substrate temperatures.

(depending on the growth temperature). The vertical error bar is the root mean square value of the distribution of  $d$ . The error bar on the composition is due to uncertainties on the amount of Ge contained in the WL (assumed to vary between 1 and 3 ML) and in the discrimination between island and substrate material. Uncertainties in the amount of deposited Ge are smaller than the above quoted errors and are not included. Because of AFM tip convolution effects [whose relevance increases with decreasing island size (increasing Ge content)], the average compositions extracted from AFM are likely to be slightly underesti-



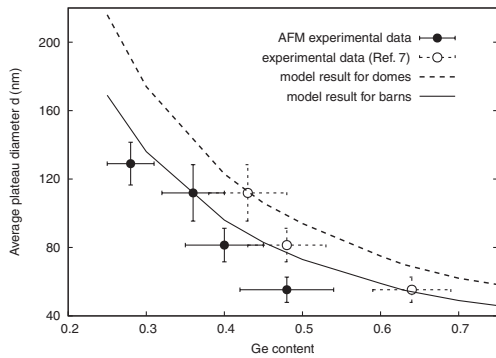


FIG. 4. Comparison between experimental data and model predictions of the island base size. The latter has been calculated for different Ge contents, both for dome-shaped islands (dashed line) and for barn-shaped ones (solid line). AFM values (full circles) at different temperatures (i.e., Ge contents) have been reported, along with independent measurements of the Ge content by x-ray scattering (open circles).

ated. We therefore added in the plot also the composition values obtained by independent X-ray diffraction measurements (open circles as taken from Ref. [7]) performed on samples grown at the same temperatures. Model predictions for domes, with aspect ratio 0.2, and barns, with aspect ratio 0.3, are displayed as dashed and continuous lines, respectively.

In spite of the uncertainties in the measurements, especially for what concerns the average composition values, we observe a better overall agreement between the experimental values for the average critical plateau size at different temperatures (full and open circles in Fig. 4) and the model prediction for the barn case (continuous line in Fig. 4), rather than for the dome case (dashed line in Fig. 4). We therefore conclude that, at growth temperatures between 620 and 800 °C, where the barns are observed, they are likely to represent the ultimate coherent island shape in the morphological evolution during deposition, when plastic relaxation sets in.

More than that, an important result of our analysis is that the critical size, as calculated on purely thermodynamic grounds, fits to the same extent the experimental data at high temperatures and the ones at low temperatures. This indicates the nucleation of the first dislocation in the island not to be delayed by activation energies larger than  $\sim kT$  at 620 °C, at variance to the common behavior in overcritical flat films [9]. This issue is in agreement to what found by Tillman and Förster [15] for  $\text{In}_{0.6}\text{Ga}_{0.4}\text{As}$  islands on GaAs, still at much smaller critical bases and one growth temperature, suggesting it to be a general property of the three-dimensional island morphology.

It is likely [9] that the highly inhomogeneous distribution of the stress components in the island, exceeding some GPa close to the island edges [see Figs. 1(b) and 2(b)], provides a homogeneous nucleation mechanism of the dislocation right at the substrate interface, at variance to the case of the flat film, where the loop is activated at

surface defects and glides subsequently towards the interface. It is not possible, at present, to calculate correctly the corresponding activation barrier, still by considering the mapping of  $E_{\text{gain}}$  in Figs. 1(c) and 2(c), it appears to be more convenient to inject a dislocation segment from the left side of the island, rather than from the top, since  $E_{\text{cost}}$ , calculated on purely geometric grounds in a fully relaxed island, is nearly the same.

We gratefully acknowledge R. Gatti and J. Stangl for helpful discussions and the financial support of a EC grant (Contract No. 012150, Strep Project D–DOT FET) and of the Cariplo Foundation.

\*Corresponding author.  
leo.miglio@unimib.it

†Present address: Institute of Semiconductor Physics, Novosibirsk, 630090, Russia.

- [1] J. Stangl, V. Holy, and G. Bauer, *Rev. Mod. Phys.* **76**, 725 (2004).
- [2] G. Medeiros-Ribeiro, A.M. Bratkovski, T.I. Kamins, D.A.A. Ohlberg, and R.S. Williams, *Science* **279**, 353 (1998).
- [3] E. Sutter, P. Sutter, and J.E. Bernard, *Appl. Phys. Lett.* **84**, 2262 (2004).
- [4] M. Stoffel, A. Rastelli, J. Tersoff, T. Merdzhanova, and O.G. Schmidt, *Phys. Rev. B* **74**, 155326 (2006).
- [5] M. Floyd *et al.*, *Appl. Phys. Lett.* **82**, 1473 (2003).
- [6] G. Capellini, M. De Seta, and F. Evangelisti, *Appl. Phys. Lett.* **78**, 303 (2001).
- [7] J. Stangl *et al.*, *Adv. Solid State Phys.* **44**, 227 (2004). The estimation of the error bars in Fig. 4 is a private communication of J. Stangl (University of Linz).
- [8] G. Medeiros-Ribeiro and R.S. Williams, *Nano Lett.* **7**, 223 (2007).
- [9] R. Hull, in *Properties of Silicon Germanium and SiGe: Carbon*, edited by Kasper and Lyutovich (Inspec., London, 2000), p. 9.
- [10] F.K. LeGoues, M.C. Reuter, J. Tersoff, M. Hammar, and R.M. Tromp, *Phys. Rev. Lett.* **73**, 300 (1994).
- [11] M. Hammar, F.K. LeGoues, J. Tersoff, M.C. Reuter, and R.M. Tromp, *Surf. Sci.* **349**, 129 (1996).
- [12] A. Rastelli, M. Stoffel, U. Denker, T. Merdzhanova, and O.G. Schmidt, *Phys. Status Solidi A* **203**, 3506 (2006).
- [13] T. Merdzhanova, S. Kiravittaya, A. Rastelli, M. Stoffel, U. Denker, and O.G. Schmidt, *Phys. Rev. Lett.* **96**, 226103 (2006).
- [14] H.T. Johnson and L.B. Freund, *J. Appl. Phys.* **81**, 6081 (1997).
- [15] K. Tillman and A. Förster, *Thin Solid Films* **368**, 93 (2000).
- [16] B.J. Spencer and J. Tersoff, *Phys. Rev. B* **63**, 205424 (2001).
- [17] J.P. Hirth and J. Lothe, *Theory of Dislocations* (Krieger, Malabar, 1992).
- [18] I.N. Remediakis, D.E. Jesson, and P.C. Kelires, *Phys. Rev. Lett.* **97**, 255502 (2006).
- [19] R. Gatti *et al.* (unpublished).